

– Supporting Information –

Interrogation of Electrocatalytic Water Oxidation

Mediated by a Cobalt Complex

Derek J. Wasylenko,^a Ryan D. Palmer,^a Eduardo Schott,^b and Curtis P. Berlinguette^{a}*

^a Department of Chemistry, University of Calgary, 2500 University Drive N.W., Calgary, Alberta,
Canada T2N-1N4

^b Departamento de Ciencias Químicas, Universidad Andres Bello, Republica 275, Santiago, Chile

Email: cberling@ucalgary.ca

Experimental Section

Synthesis.

PY5 (2,6-bis(bis-2-pyridyl)-methoxymethane)pyridine)^[1-2] and $[\text{Co}^{\text{II}}(\text{PY5})(\text{OH}_2)](\text{ClO}_4)_2$ (**1**)^[3] were prepared as previously described. All reagents (including those used for preparation of solutions) were purchased from either Sigma Aldrich or Alfa Aesar and used as received unless otherwise noted. D_2O (99%) was purchased from Cambridge Isotope Laboratories.

Physical Methods.

Electrochemical measurements were recorded using Milli-Q H_2O ($R = 18.2 \text{ M}\Omega$) with a Princeton Applied Research VersaStat 3 potentiostat, a CH Instruments glassy carbon working electrode (area = 0.071 cm^2), a Pt wire counter electrode and home-made $[\text{Ag}]/[\text{AgCl}]$ or $[\text{Cu}]/[\text{CuSO}_4]$ reference electrodes, calibrated against both a commercial (PAR K0077) saturated calomel electrode (SCE) and against the $[\text{Fe}^{\text{III}}(\text{CN})_6]^{3-}/[\text{Fe}^{\text{II}}(\text{CN})_6]^{2-}$ redox couple in 1 M HClO_4 (0.72 V vs NHE).^[4] Chronopotentiometry experiments were used to verify the stability of the reference electrodes. Potentials reported herein are referenced to a normal hydrogen electrode (NHE) according to the calibration. The glassy carbon working electrode was polished between runs with an alumina slurry (0.05 micron particle size) on a nylon mesh to achieve a mirror finish, thoroughly rinsed with water followed by successive sonication in H_2O , methanol and dichloromethane to remove residual materials. The working electrodes were then further conditioned by cycling the electrode between 0 and 1.6 V vs NHE for 5 to 10 cycles in blank electrolyte until an acceptably stable voltammogram was achieved. Buffer solutions were used to achieve the various pH ranges; *i.e.*, a NaOAc/HOAc buffer (0.1 M) solution at $\text{pH} < 4$, and a phosphate buffer (0.1 M KH_2PO_4 or 0.1 M K_2HPO_4) at higher pH levels. The pH was adjusted by adding aliquots of 5 M KOH or 5 M HNO_3 prepared from Milli-Q H_2O . Scan rate dependent studies were conducted at $n = 20, 50, 100, 250$ and 500 mVs^{-1} . Solution resistance was determined to be negligible under our conditions and therefore iR compensation was not applied.

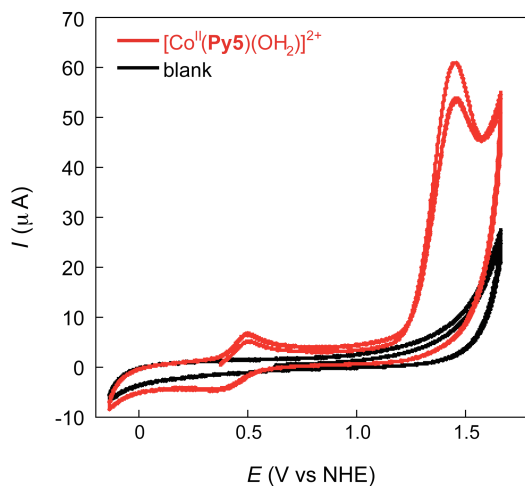


Figure S1. Cyclic voltammogram (CV) of **1** in 0.1 M KPi pH 9.2 at a scan rate of 50 mVs⁻¹. (The working electrode is GC (3 mm) with a Pt wire counter electrode and Cu/CuSO₄ reference electrode.) Reproduced with permission from the Royal Society of Chemistry.³

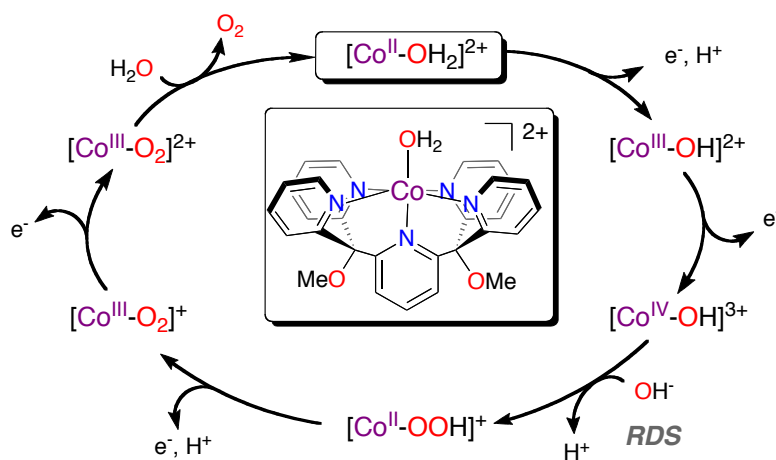


Figure S2. Proposed catalytic water oxidation pathway mediated by **1**.

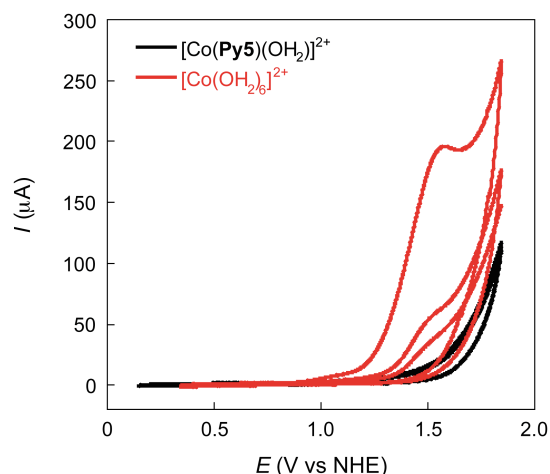


Figure S3. Homogeneity test of electrode surface following catalysis by **1**. This figure depicts the cyclic voltammetric response (scan rate = 10 mV s^{-1}) of the glassy carbon working electrode (diameter = 3 mm) in a blank electrolyte (0.1 M KPi) following two anodic cycles from 0 - 1.8 V vs NHE (ending at 1.8 V; scan rate = 10 mVs^{-1}) in 1 mM solutions of $[\text{Co}(\text{OH}_2)_6](\text{ClO}_4)_2$ (red) or $[\text{Co}(\text{PY5})(\text{OH}_2)](\text{ClO}_4)_2$ (black). The electrode was taken out of the solution, thoroughly rinsed with distilled, deionized water and left to air-dry prior to further testing. After anodic cycling in the $[\text{Co}(\text{OH}_2)_6]^{2+}$ solution, a blue film is visible on the electrode surface; this same film is not visible after anodic cycling of the $[\text{Co}(\text{PY5})(\text{OH}_2)]^{2+}$ solution. Taken together with the lack of any significant features in the cyclic voltammogram of the electrode after anodic cycling in a $[\text{Co}(\text{PY5})(\text{OH}_2)]^{2+}$ solution (black line) suggests that the formation of $\alpha\text{-CoO}_x$ is not promoted on the electrode surface following anodic cycling in the $[\text{Co}(\text{PY5})(\text{OH}_2)]^{2+}$ solution. Reproduced with permission from the Royal Society of Chemistry.³

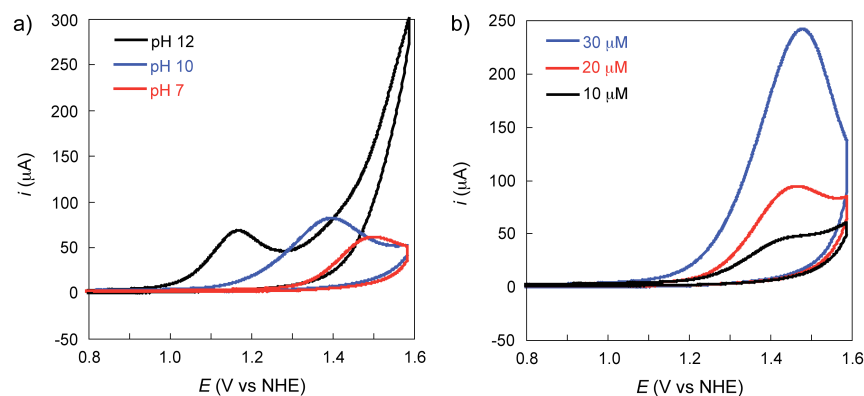


Fig. S4. (a) CVs recorded on solutions of $[\text{Co}(\text{OH}_2)_6](\text{ClO}_4)_2$ at various (a) pH levels ($[\text{Co}^{2+}] = 10 \mu\text{M}$) and (b) Co(II) concentrations (pH = 9.2). (scan rate = 50 mVs^{-1} ; GC (3 mm) working electrode; Pt wire counter electrode; and Cu/CuSO_4 reference electrode.)

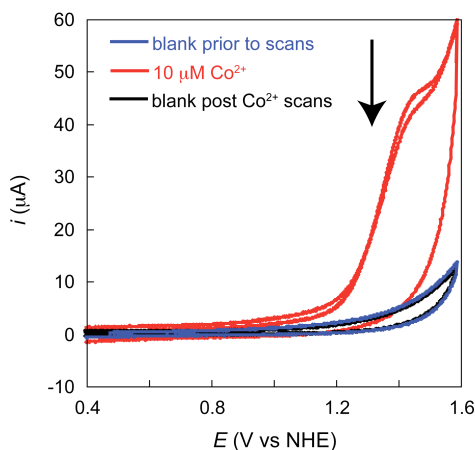


Figure S5. Homogeneity test of electrode surface from dilute $[\text{Co}^{\text{II}}(\text{OH}_2)_6](\text{ClO}_4)_2$ solutions. This figure depicts the cyclic voltammetric response (scan rate = 20 mVs^{-1}) of the glassy carbon working electrode (diameter = 3 mm) in a blank electrolyte (0.1 M KPi) prior to adding Co^{2+} (blue) and following two anodic cycles from 0 - 1.6 V vs NHE (ending at 1.6 V; scan rate = 20 mVs^{-1}) in $10 \mu\text{M}$ solutions of $[\text{Co}(\text{OH}_2)_6](\text{ClO}_4)_2$ (red) and after rinsing the electrode with H_2O then scanning in blank electrolyte (black). The data suggests that the formation of an $\alpha\text{-CoO}_x$ film is not promoted on the electrode surface following anodic cycling, but is more likely to be catalytically active nanoparticles formed in solution near the electrode.

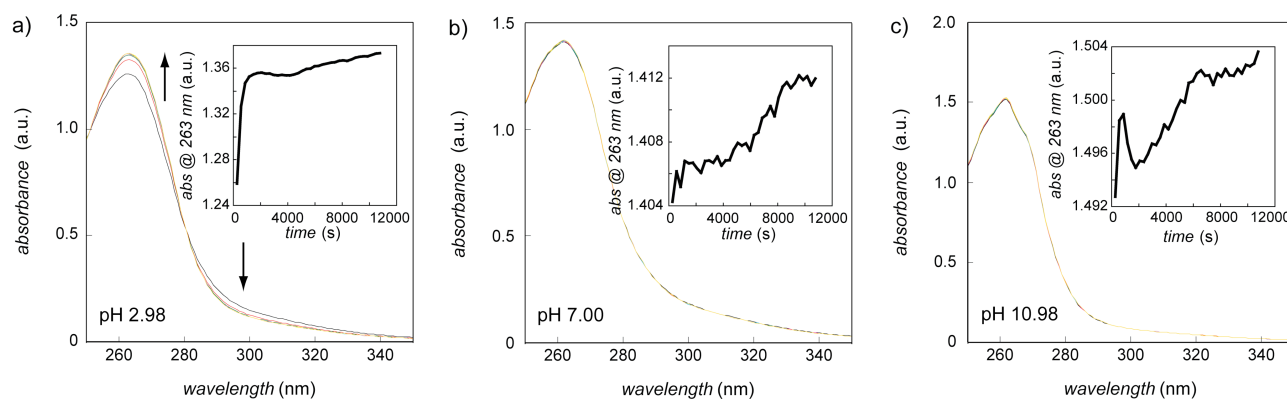


Figure S6. Time-dependent UV-vis spectra of 0.1 M KPi solutions of **1** ($[1] \sim 100$ mM) at (a) pH 2.98; (b) pH 7; and (c) pH 10.98 (pH was adjusted with 5 M HNO_3 or KOH solutions). *Insets:* Absorbance at 263 nm versus time ($t = 5$ min to 3 h). The temporal trace reveals absorbance changes of ~ 0.1 a.u. at pH 2.98 over the 3-h time period, while nominal absorbance changes (~ 0.01 a.u.) are observed in neutral and basic conditions. This data indicates Co^{2+} is not being leached from **PY5** over 3 h at pH 7 and 10.98.

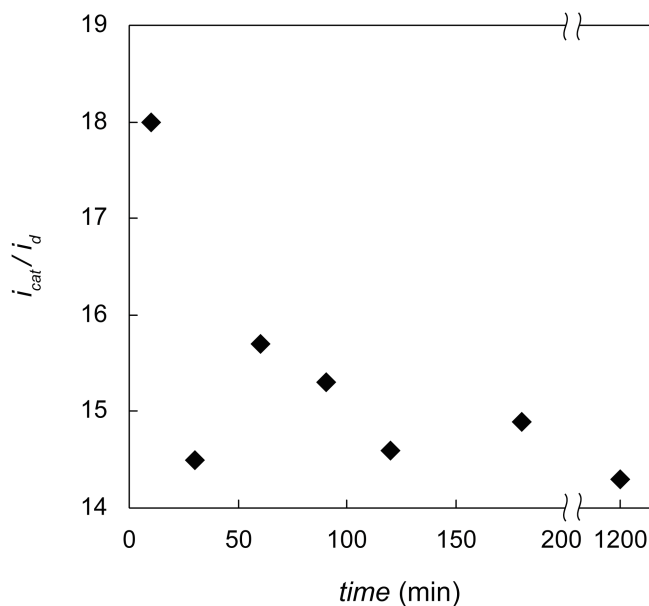


Figure S7. Ratio of catalytic current (i_{cat}) to the diffusional current of the Co(III)/Co(II) couple (i_d) for **1** as a function of time in solution (0.1 M KPi, pH 9.2, scan rate = 20 mVs^{-1}). If Co^{2+} is being leached from the **PY5** ligand over time, the ratio would be expected to grow larger (see Figure S4b); however, this is not observed.

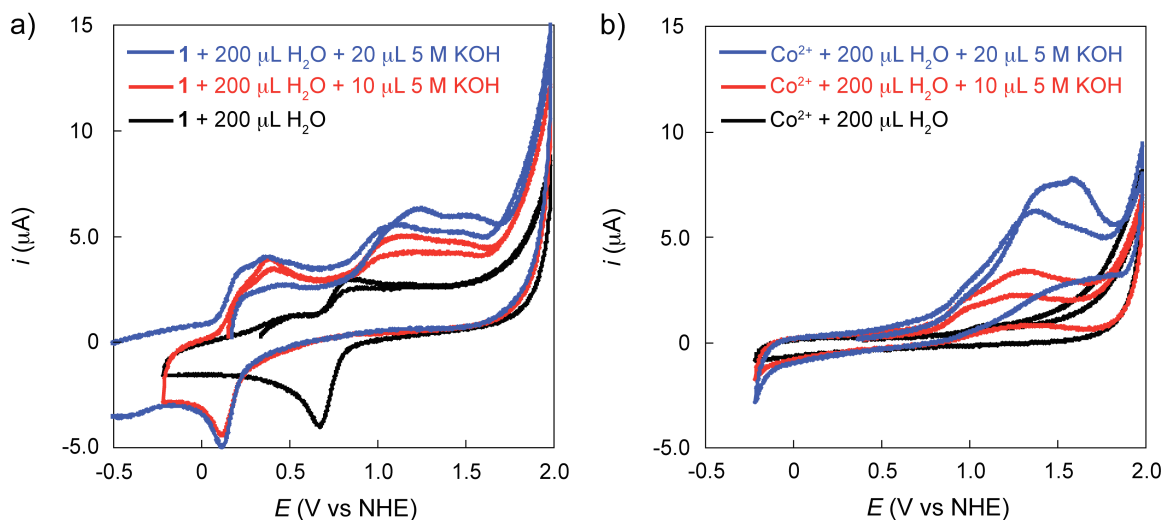


Figure S8. Cyclic voltammograms of a (a) 0.5 mM solution of **1** and (b) 10 μM solution of $[\text{Co}(\text{OH}_2)_6](\text{ClO}_4)_2$ measured in 0.1 M $(\text{Bu}_4\text{N})(\text{BF}_4)$ /propylene carbonate (PC) solution with added H_2O and 5 M KOH. (Scan rate = 20 mVs^{-1} ; working electrode = 3 mm glassy carbon; counter electrode = Pt; reference electrode = Cu/CuSO₄.)

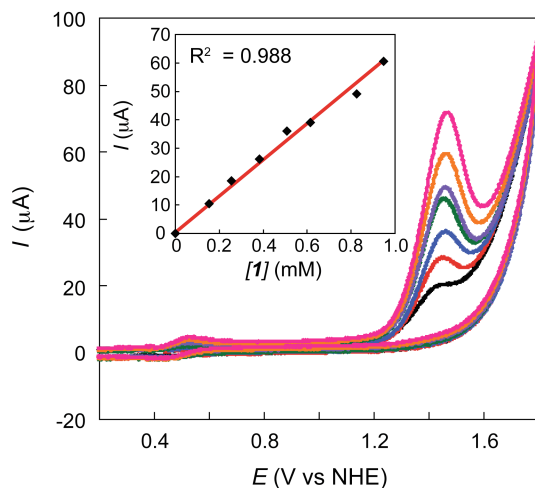


Figure S9. Cyclic voltammograms recorded in 0.1 M KPi buffer (pH 9.2, $n = 10 \text{ mVs}^{-1}$) demonstrating the dependence of the catalytic current ($E_{\text{p,a}} = 1.45 \text{ V vs NHE}$) on $[\mathbf{1}]$; *inset*: the background corrected catalytic currents as a function of $[\mathbf{1}]$ indicating reactivity that is first-order in $[\mathbf{1}]$.

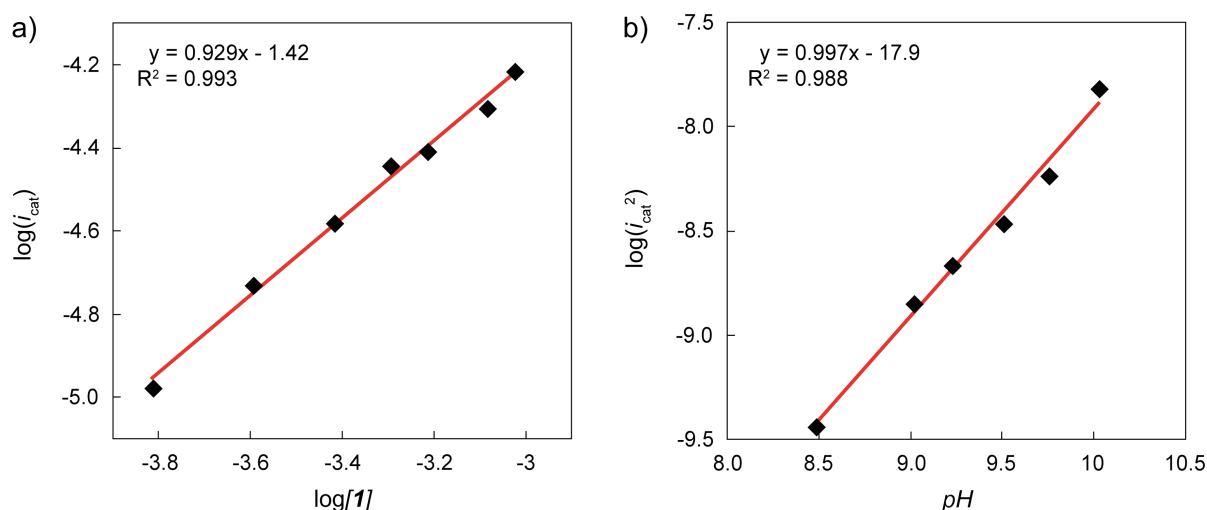


Figure S10. (a) $\log(i_{\text{cat}})$ vs. $\log[1]$ demonstrating first-order behaviour in $[1]$. (b) pH dependence of $\log(i_{\text{cat}}^2)$ at constant $[1]$ (0.5 mM) demonstrating that i_{cat} is dependent on $[\text{OH}^-]$. i_{cat} values were determined at a scan rate of 10 mVs^{-1} . The relationship between i_{cat}^2 and $[\text{OH}^-]$ is derived from the equation, $i_{\text{cat}} = nFA[1]_0(k_{\text{obs}}D_1)^{1/2}$ where $k_{\text{obs}} = k_{\text{cat}}[\text{OH}^-]$ and the other terms are defined in the main text.

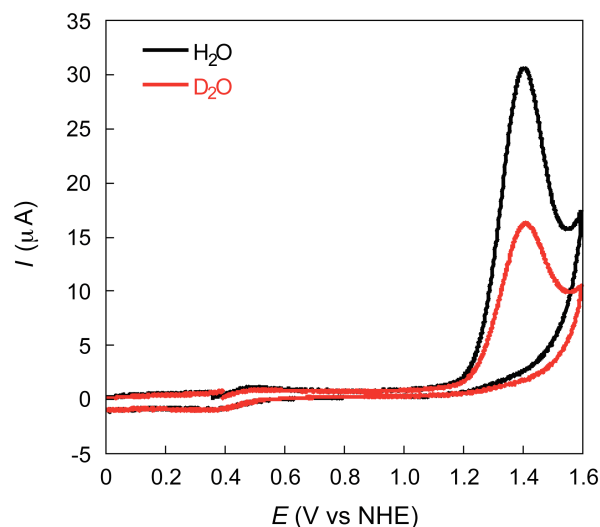


Figure S11. Cyclic voltammograms of **1** recorded in 0.1 M KPi buffered (pH 9.2, $n = 20 \text{ mVs}^{-1}$) D_2O and H_2O solutions; $[1] = 0.4 \text{ mM}$. The H/D kinetic isotope effect was determined to be 4.7. (The working electrode is GC (3 mm) with a Pt wire counter electrode and Ag/AgCl reference electrode; $[1] = 0.4 \text{ mM}$).

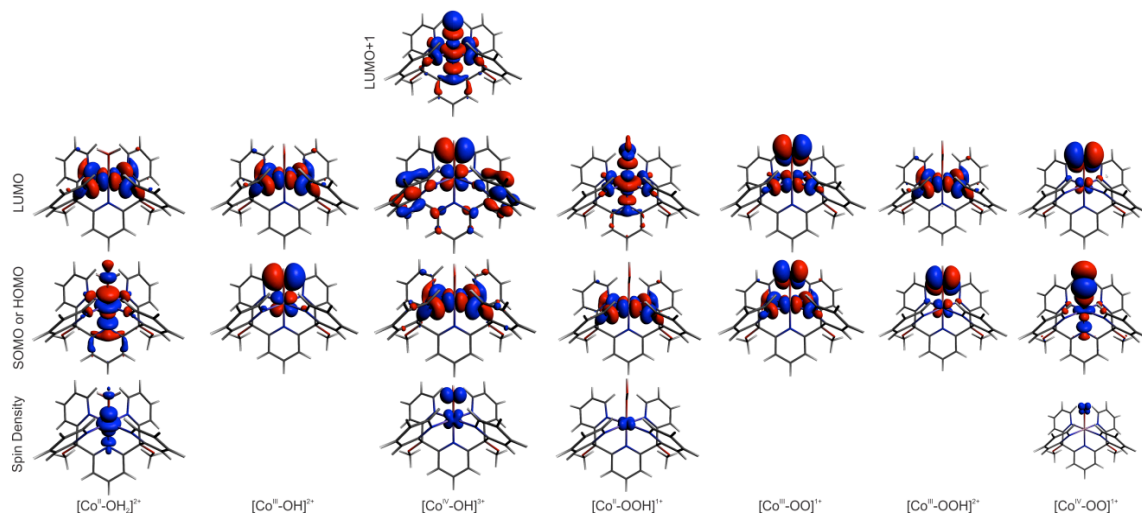


Figure S13. Plots of the frontier molecular orbitals associated with the proposed catalytic intermediates in Figure S2. The spin densities are provided for species with unpaired electrons.

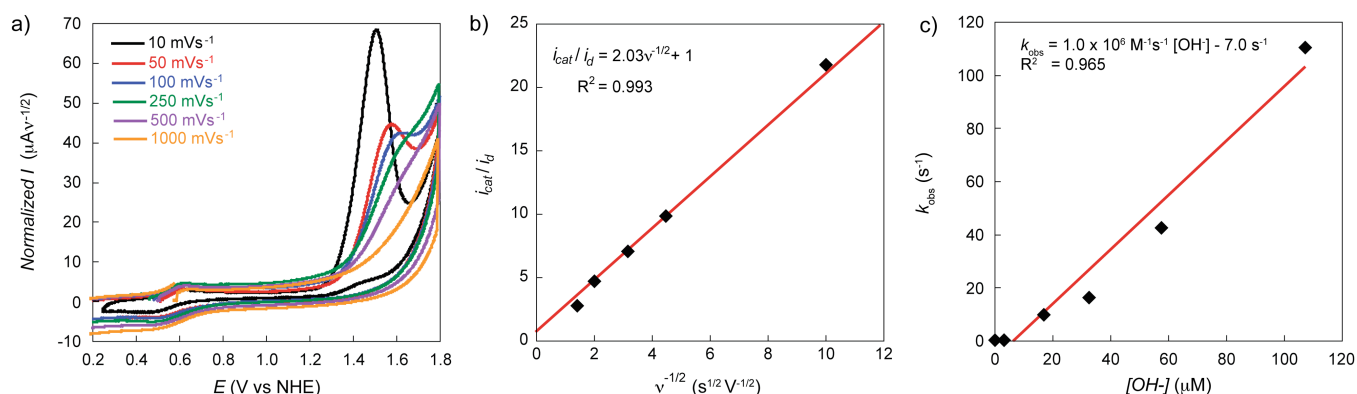


Figure S13. (a) Cyclic voltammograms of **1** recorded in 0.1 M KPi buffer (pH 9.2) demonstrating the dependence of the normalized i_{cat} ($E_{p,a} = 1.4$ - 1.6 V vs NHE) to the scan rate. (b) Background-corrected ratio of i_{cat} and i_d as a function of the negative root of the scan rate in accordance with $i_{cat}/i_d = 2.241(n_c/n_d)^{3/2}(k_{obs}RT/Fv)^{1/2}$. (c) Plot of k_{obs} versus $[OH^-]$ used to extract the second-order rate constant, k_{cat} . (The working electrode is GC (3 mm) with a Pt wire counter electrode and Cu/CuSO₄ reference electrode.) The k_{obs} values were extracted by comparing the ratios of i_{cat} [Eq. (3); n_{cat} = number of electrons transferred during the catalytic event (*i.e.*, 4); F = Faraday constant, A = electrode surface area; $[1]_0$ = bulk concentration of **1**; D_1 is the diffusion coefficient] to the diffusional currents [$i_d = 0.4463nFA[1]_0n_d^{3/2}(vFD_1/RT)^{1/2}$; n_d = number of transferred electrons associated with the diffusional couple; R = universal gas constant; T = temperature; and v = scan rate in Vs⁻¹] of the $[Co^{III}\text{-OH}]^{2+}/[Co^{II}\text{-OH}_2]^{2+}$ couple to yield $i_{cat}/i_d = 2.241(n_{cat}/n_d)^{3/2}(k_{obs}RT/vF)^{1/2}$.

This procedure yields k_{obs} values that range from 0.40 s^{-1} at pH 7 to 110 s^{-1} at pH 10.5. These values are notable because they would represent the highest values reported to date for any synthetic water oxidation catalyst if there is no contribution from Co-oxide NPs; however, we cannot rule out the presence of NPs artificially inflating these values.

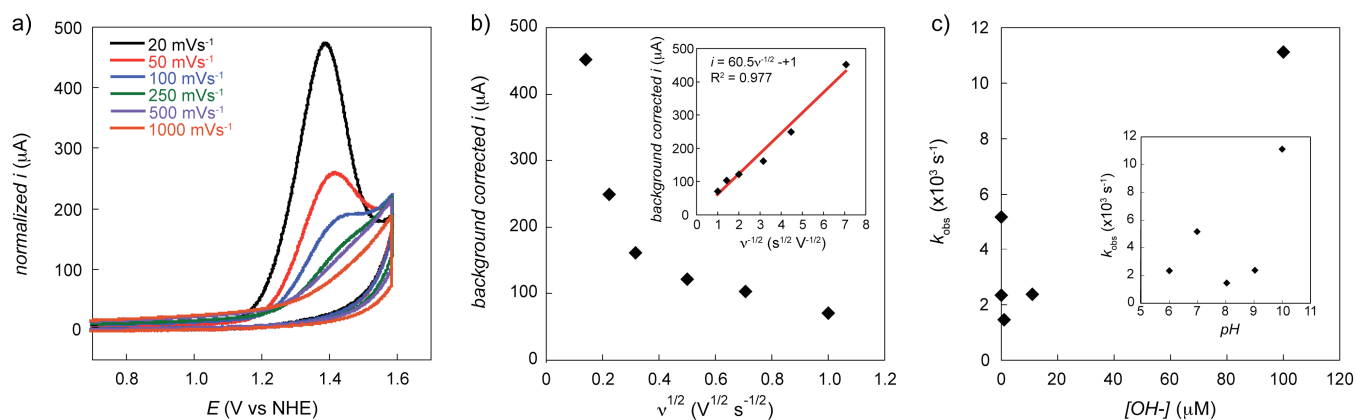


Figure S14. (a) Cyclic voltammograms of $[\text{Co}^{\text{II}}(\text{OH}_2)_6](\text{ClO}_4)_2$ (10 μM) recorded in 0.1 M KPi buffer (pH 9.2) demonstrating the dependence of the normalized i_{cat} ($E_{\text{p,a}} = 1.4\text{--}1.6$ V vs NHE) to the scan rate. (b) Background corrected i_{cat} as a function of $v^{1/2}$ demonstrating that i_{cat} is not a result of a diffusional process and is consistent with a chemical reaction coupled to the electron-transfer reaction(s). *Inset:* A similar treatment of the data where background-corrected i_{cat} is plotted as a function of $v^{-1/2}$ via a similar treatment of the data in Figure S13b yields a linear slope. *We caution that the equation in the caption of Fig. S13b does not apply to this case because i_d does not exist; this plot is only added as a qualitative comparison to Figure S13b for the reader.* (c) Plot of k_{obs} versus $[\text{OH}^-]$ for Co^{2+} in 0.1 M KPi buffer. (*Inset:* Plot of k_{obs} as a function of pH provided only as an alternative representation of the data.) Note the significant difference from Figure S13c. (The working electrode is GC (3 mm) with a Pt wire counter electrode and Cu/CuSO₄ reference electrode.) The “ k_{obs} values” were extracted using Equation 3 in the main text, where the diffusion coefficient for $\text{Co}^{2+} = 1.2 \times 10^{-5} \text{ cm}^2 \text{ s}^{-1}$.^[5] This procedure yields k_{obs} values that range from 1500 s^{-1} to 11000 s^{-1} using the aforementioned method. The significant response of 10 μM concentrations of Co^{2+} may indicate that nanoparticles with very high surface areas are being formed and catalyze water oxidation. Dramatic effects on rates of catalysis using cobalt oxide films has been documented and is highly dependent on surface area and size.^[6,7]

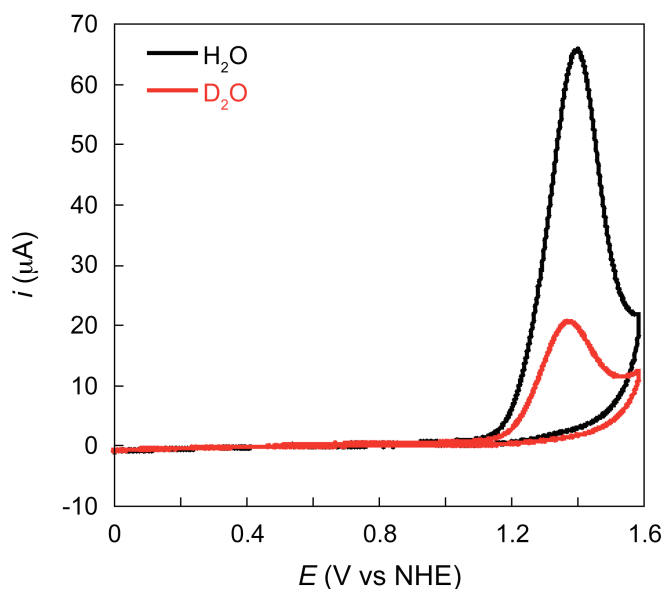


Figure S15. Cyclic voltammograms of Co^{2+} recorded in 0.1 M KPi buffered (pH 9.2, $n = 20 \text{ mVs}^{-1}$) D_2O and H_2O solutions; $[\text{Co}^{2+}] = 10 \text{ } \mu\text{M}$. The H/D kinetic isotope effect was determined to be 10.8 using equation 3 from the manuscript. (The working electrode is GC (3 mm) with a Pt wire counter electrode and Ag/AgCl reference electrode; $[\mathbf{1}] = 0.4 \text{ mM}$).

-
- [1] M.E. de Vries, R.M. La Crois, G. Roelfes, H. Kooijman, A.L. Spek, R. Hage, B.L. Feringa, *Chem. Commun.* 1997, 1549.
 - [2] R. T. Jonas, T. D. P. Stack, *J. Am. Chem. Soc.* 1997, **119**, 8566.
 - [3] D. J. Wasylenko, C. Ganesamoorthy, J. Borau-Garcia, C. P. Berlinguette, *Chem. Commun.* 2011, **47**, 4251.
 - [4] A. J. Bard, L. R. Faulkner, *Electrochemical Methods: Fundamentals and Applications*, 2nd ed., Wiley, New York, 2001.
 - [5] A. C. S. Ribeiro, V. M. M. Lobo, J. J. S. Natividade, *J. Chem. Eng. Data*, 2002, **47**, 539.
 - [6] B. S. Yeo, A. T. Bell, *J. Am. Chem. Soc.* 2011, **133**, 5587.
 - [7] A. J. Esswein, M. J. McMurdo, P. N. Ross, A. T. Bell, T. D. Tilley, *J. Phys. Chem. C* 2009, **113**, 15068.